SAND2023-04203C

Oxygen non-stoichiometry and point defect equilibria in $(La_{1/6}Pr_{1/6}Nd_{1/6}Gd_{1/6}Ba_{1/6}Sr_{1/6})MnO_{3-\delta}$

Sean R. Bishop[a], Dawei Zhang[b], Cijie Liu[c], Wei Li[c], Perla A. Salinas[a], Andrew I. Smith[a], Eric N. Coker[a], Héctor A. De Santiago,[c] Xingbo Liu[c], Anthony H. McDaniel[d], and Jian Luo[b,e]

[a]Sandia National Laboratories, Albuquerque, NM 87123, United States
[b]Program of Materials Science and Engineering, University of California San Diego, La Jolla, CA 92093, United States
[c]Department of Mechanical and Aerospace Engineering, Benjamin M. Statler College of Engineering and Mineral Resources, West Virginia University, Morgantown, WV 26506, United States
[d]Sandia National Laboratories, Livermore, CA 94550, United States
[e]Department of NanoEngineering, University of California San Diego, La Jolla, CA 92093, United States

In this work, the A-site of the common SOFC cathode $La_{0.8}Sr_{0.2}MnO_{3-\delta}$ (LSM) is modified with additional lanthanide and alkali elements, resulting in the composition $(La_{1/6}Pr_{1/6}Nd_{1/6}Gd_{1/6}Ba_{1/6}Sr_{1/6})MnO_{3-\delta}$. We show that the amount of oxygen released during reduction measured by thermo-gravimetric analysis is significantly greater for this “high entropy” perovskite oxide (HEPO) in comparison with $La_{2/3}Sr_{1/3}MnO_{3-\delta}$, the latter having the same amount of total acceptor dopant and with a similar average A-site radius. The origins of enhanced reduction will be discussed.

Introduction

Compositionally complex oxides (CCOs), also referred to as high entropy oxides, have several different cations (typically 5 or more) occupying a single site. CCOs have shown unique dielectric, ionic conductivity, and thermal conductivity properties, in addition to promising electrochemical properties for solid oxide fuel cells (SOFCs) [1,2]. In this work, the A-site of the common SOFC cathode $La_{0.8}Sr_{0.2}MnO_{3-\delta}$ (LSM) is modified with additional lanthanide and alkali elements, resulting in the composition $(La_{1/6}Pr_{1/6}Nd_{1/6}Gd_{1/6}Ba_{1/6}Sr_{1/6})MnO_{3-\delta}$. The oxygen non-stoichiometry (δ) measured by thermogravimetric analysis in ~10^{-5} – 1 atm O_2 at 1400 °C is presented and the point defect equilibria analysis is discussed. Comparisons with existing high temperature experimental and modeling studies on LSM are also be discussed.

Experimental

$(La_{1/6}Pr_{1/6}Nd_{1/6}Gd_{1/6}Ba_{1/6}Sr_{1/6})MnO_{3-\delta}$ (HEPO) and $La_{2/3}Sr_{1/3}MnO_{3-\delta}$ (LSM33) were fabricated by conventional solid state synthesis. All powder precursors were ball milled and annealed at 1300 ºC in air for 10 h. The synthesized powders were ground by using a mortar and pestle and then re-annealed at 1400 ºC for 10 h to improve homogeneity.

Thermo-gravimetric analysis (TGA) was performed using a Netzsch STA 449 F1. Oxygen partial pressure (pO_2) was controlled by mixing oxygen, argon, and pre-mixed 1100 ppm O_2 in argon and measured on the exhaust side of the instrument using a Zirox ZR5 oxygen sensor. Approximately 500 mg of sample was used in TGA measurements. Corrections for buoyancy were performed using a crucible filled with coarse alumina powder to approximately the same volume of powder as measured samples.

Results and Discussion

The following point defect relationships for the reduction reaction (equation 1) and charge disproportionation reaction (equation 2) have been used to describe oxygen non-stoichiometry of LSM.

$$2Mn_{Mn}^{\cdot} + O_O^x = 2Mn_{Mn}^x + V_O^{\cdot\cdot} + \frac{1}{2}O_2(g) \qquad [1]$$

$$2Mn_{Mn}^x = Mn_{Mn}^{\cdot} + Mn_{Mn}' \qquad [2]$$

where $Mn_{Mn}^{\cdot}$, Mn_{Mn}^x, Mn_{Mn}', O_O^x, and $V_O^{\cdot\cdot}$ represents a hole (i.e., Mn^{4+}), a neutral (with respect to the crystal lattice) Mn cation (i.e., Mn^{3+}), an electron (i.e., Mn^{2+}), an oxygen on an oxygen site, and an oxygen vacancy, respectively. When $\delta = 0$, the average charge of Mn is 3+, however, with increasing temperature reaction 2 is expected to move to the right (analogous to thermal generation of electrons and holes) and thus both charged Mn species ($Mn_{Mn}^{\cdot}$ and Mn_{Mn}') play a role in defect equilibria. Upon exposure to lower pO_2, equation 1 moves to the right to generate oxygen vacancies, Mn_{Mn}^x, and Mn_{Mn}' (via equation 2). An example of fitting the mass action equations for equation 1 and 2 to 1300 – 1500 °C LSM non-stoichiometry data has been presented by [3]. Acceptor doping by substitution of La with Sr (Sr_{La}') is charged compensated by the formation of positive point defects, i.e., $V_O^{\cdot\cdot}$ and $Mn_{Mn}^{\cdot}$, and for low Sr content (~<0.1 site fraction), oxygen excess has been observed, with additional point defects (i.e., cation vacancies) required in analysis [4].

Increasing Sr acceptor concentration in LSM has been shown to increase δ for the same temperature and pO_2 [4]. In the present work, δ increases at 1400 °C from the studied LSM33 to previously reported LSM40 (0.4 site fraction Sr) [3], as expected and shown in figure 1. Also shown in the figure, $(La_{1/6}Pr_{1/6}Nd_{1/6}Gd_{1/6}Ba_{1/6}Sr_{1/6})MnO_{3-\delta}$ (HEPO) (having the same total acceptor content as LSM33) shows a significantly greater δ, and even greater δ than that for LSM40. Similar behavior was observed at 1200 °C (to be presented in an upcoming publication).

The 6% larger ionic radius of Sr [6] increases the lattice parameter and thus bond length with increasing Sr, which may lead to weaker bonding and increased reducibility, consistent with the above trend with Sr content. In contrast, substitution with Ca (nearly the same size as La) for La has shown less reducibility as compared to the much larger Sr [7]. However, for the HEPO material, the average A-site ionic radius is only ~0.5% smaller than that for LSM33 (based on 8-fold coordination as 12-fold is not available for all A-site constituents), and thus the observed significantly greater reducibility can not be explained by a significant change in average A-site size. Similar lattice parameters for both LSM33 and HEPO (rhombohedral structure ($R\bar{3}c$) a = 5.49747(1) Å, c = 13.36141 (1) Å and a = 5.48253 (4) Å, c = 13.4258 (3) Å, respectively) were observed from Rietveld refinement of X-ray diffraction patterns. Instead, the enhanced reducibility may be related to highly variable local A-site ionic radii.

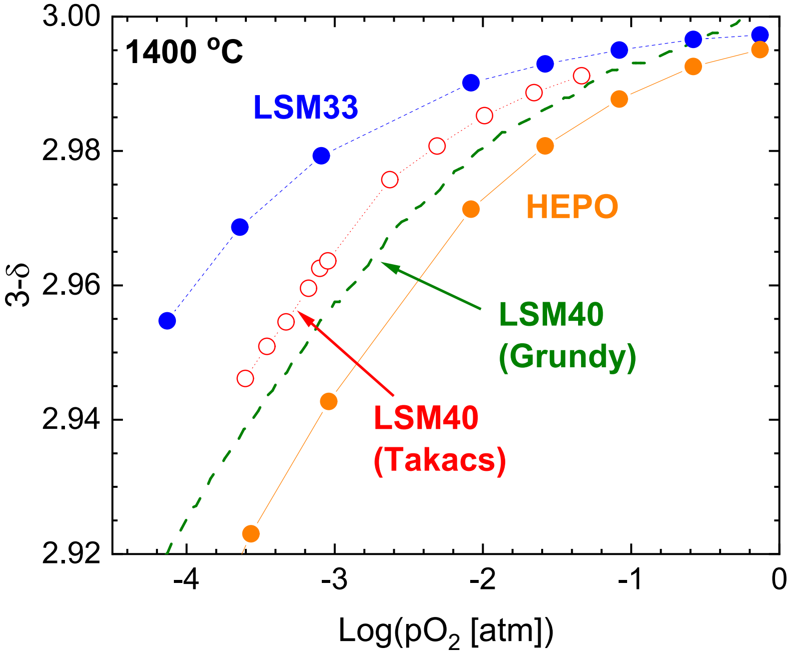

Figure 1. Oxygen non-stoichiometry measured for LSM33 and HEPO compared with the literature for LSM40 measurements (Takacs [3]) and modeling (Grundy [5]).

Summary

$(La_{1/6}Pr_{1/6}Nd_{1/6}Gd_{1/6}Ba_{1/6}Sr_{1/6})MnO_3$ is shown to have a much greater reducibility than a corresponding LSM with the same approximate average A-site ionic radius and acceptor dopant content. The enhanced reducibility may be related to highly variable local A-site ionic radii.

Acknowledgements

Sandia National Laboratories is a multimission laboratory managed and operated by National Technology & Engineering Solutions of Sandia, LLC, a wholly owned subsidiary of Honeywell International Inc., for the U.S. Department of Energy's National Nuclear Security Administration under contract DE-NA0003525. This paper describes objective technical results and analysis. Any subjective views or opinions that might be expressed in the paper do not necessarily represent the views of the U.S. Department of Energy or the United States Government.

References

1. Y. Xu, et al., *J. Adv. Ceram.*, **11** 794 (2022).
2. J. Dabrowa, et al., *J. Mater. Chem. A*, **8** 24455 (2020).
3. M. Takacs, et al., *Acta Mater.*, **103** 700 (2016).
4. J. Mizusaki, et al., *Solid State Ionics*, **129** 163 (2000).
5. A. N. Grundy, B. Hallstedt, and L. J. Gauckler, *CALPHAD*, **28** 191 (2004).
6. R. D. Shannon, *Acta Cryst.*, **A32** 751 (1976).
7. L. Rørmark, et al., *J. Mater. Chem.*, **12** 1058 (2002).